Wavefront sensor for the Large Binocular Telescope laser guide star facility

L. Busoni[a], S. Esposito[a], S. Rabien[b], M. Haug[b], J. Ziegleder[b], G. Hölzl[b]

[a]INAF-Osservatorio Astrofisico di Arcetri, L.go Fermi 5, 50125 Firenze, Italy
[b]Max-Planck-Institut für Extraterrestrische Physik, 85748 Garching, Germany

ABSTRACT

A laser guide star facility is currently being planned for the LBT. The first step of the program aims at the implementation of a ground layer adaptive optics (GLAO) system tailored on the wide-field imager / multi-object spectrograph LUCIFER having a 4x4' FoV. The current design is based on multiple Rayleigh guide stars arranged in a 2-5 arcmin angular radius constellation. A future update path toward small-field diffraction limited performances is foreseen using a hybrid system of sodium and Rayleigh beacons promising lower power requirements for the sodium laser. In this paper we present the estimated performances for both the GLAO and the hybrid implementations and we introduce the wavefront sensors opto-mechanical design . Simulations of the GLAO system show an expected gain in FWHM and encircled energy of 1.5-3 (depending on atmospheric turbulence profiles) with a FWHM variation over LUCIFER FoV below 10% and point out the role of such a GLAO system as PSF stabilizer both over the FoV and with respect to seeing temporal variations. Results of simulations for the hybrid configurations will be presented.

Keywords: Wavefront sensor, Laser Guide Star, Large Binocular Telescope, Ground Layer Adaptive Optics.

1. INTRODUCTION

The LBT laser guide star program will equip the Large Binocular Telescope with a Rayleigh Ground Layer AO system that will provide uniform, full-field correction to LUCIFER, a wide-field imager/multi-object spectrograph having a 4x4 arcmin FoV. The program is multi-staged: the LBT partners asked for a prompt implementation of a reliable, low maintenance system with low risks and minimized changes to existing telescope systems, capable of operating significantly above median atmospheric conditions. In a second time, the existing Rayleigh GLAO system will be upgraded to reach diffraction-limited performances. The current baseline for the upgraded system is made of an hybrid system of Rayleigh and sodium beacons that seems capable of reach high Strehl ratio in J –K bands using a low-power sodium laser complementary to the Rayleigh GLAO system.

In section 2 we present a summary of system performance simulations performed with the aim of screening the parameter space and providing guidelines for the definition of the GLAO wavefront sensor baseline configuration. The simulations suggest that the GLAO system will increase the performance in both resolution and energy concentration of a factor 2-3. In section 3 the optical design of the GLAO Shack Hartmann wavefront sensor is described. The design make use of a periscope to bring the LGS beams close and parallel to each other and to collimate them. A single collimator and lenslet array is used to accommodate the 4 spot patterns on a single CCD. In section 4 an upgraded version of the Rayleigh GLAO facility capable of on-axis diffraction-limited performances is outlined. We propose an hybrid system where the firstly implemented Rayleigh GLAO system samples the strong turbulence above the ground and a sodium laser measures the high altitude turbulence. The key point of the technique is the consideration that the residual high altitude turbulence after the GLAO correction corresponds to effective r0 value that are ~3 times larger than the full-atmosphere values. As a consequence the sodium wavefront sensor can use subapertures that are ~10 times larger in area than in the case of a typical full-atmosphere sodium laser and this is immediately reflected in a similar amount of laser power gain. Preliminary

Adaptive Optics Systems, edited by Norbert Hubin, Claire E. Max, Peter L. Wizinowich,
Proc. of SPIE Vol. 7015, 701556, (2008)
0277-786X/08/$18 · doi: 10.1117/12.789063

simulations of such a systems predicts on-axis diffraction-limited performance in J to K band for almost all the atmospheric profiles used in this study.

2. NUMERICAL SIMULATION

The goal of simulations is to provide guidelines for the design of the wavefront sensors by comparing the performance of the system under different configurations. Since we want to focus on screening the parameter space and on defining a baseline configuration, the effects that are common to all the configurations, e.g. the ones related to the deformable mirror like bandwidth or loop-delay, are ignored.

2.1 Model assumptions

Simulations are performed in open-loop. A typical simulation run is made of 100 independent short-exposures, sampling a square 4x4' FoV on a 5x5 grid. The PSFs of each short-exposure are summed to provide a long-time exposure that is analyzed to extract the FWHM and the Ensquared Energy in a 0.25" square pixel (EE in the following).

The baseline configuration for simulations assumes 4 Rayleigh stars at 12km, gated 100m and arranged on a 4' radius circle. A list of code features that are worth to be noted follows:

- Atmospheric model: phase-screens are generated using the PSG package from the CAOS software [11]. Screens are 1024x1024 pixels, sampled at 0.046m/px with infinite outer scale. The atmosphere is sliced in 12 discrete layers. Turbulence strength for each layer is provided by the turbulence profiles measured on Mt Graham [3] grouped in 4 reference profiles named '25', '50', '75', 'bad' having 0.56, 0.68, 0.82, 1.2 arcsec seeing respectively (see Table 1 for r0 values).
- Geometrical model to account for spot elongation: a simple paraxial telescope is modeled to compute the size of the elongated spot. Both gating thickness and off-axis projection contribute to the elongation of the spot and both contributions are taken into account. Spot elongation (size and direction) is used in conjunction with the spot size due to seeing to create a kernel image for each subaperture of the SH WFS. In each subaperture of the WFS, the kernel image is convolved to the LGS image and the resulting image is used to compute the slopes.
- Focal anisoplanatism: a LGS is supposed to be a point-like source located at a given height and direction. LGS light is assumed to follow a cone while back-propagating towards the telescope.

Table 1r0 values [m] for the 4 atmospheric profiles used in this study

Altitude [m]	125	375	625	875	1125	1375	1675	3000	5000	10000	15000	20000
25%	0.27	0.56	1.04	2.35	2.8	2.15	1.85	0.86	1.27	1.05	1.36	3.7
50%	0.24	0.48	0.90	2.03	2.42	1.85	1.59	0.74	0.92	0.76	1.2	3.12
75%	0.21	0.44	0.81	1.83	2.18	1.67	1.44	0.61	0.69	0.58	1.09	3.11
bad	0.14	0.28	0.52	1.18	1.41	1.08	0.93	0.84	0.56	0.22	0.92	2.3

- The deformable mirror is supposed to perfectly follow the commands with instantaneous response time. The DM is optically conjugated at 0m.
- Vignetting of LGS beams by M3 is taken into account. Input on vignetted subapertures for each LGS is provided by ZEMAX analysis.

- Shack-Hartmann WFS: 15x15 subapertures, FoV 5.3”. RON=0. Centroid algorithm. The tip/tilt of the LGS wavefronts is subtracted simulating a recentering loop in the laser launch system.
- Tip Tilt WFS: is simulated as a 1x1 SH. The TT WFS is fed with the wavefront corrected for the GL as sensed by the SH WFS.
- Reconstruction and control: 150 Karhunen-Loeve modes are corrected. No reconstruction time delay is considered.

2.2 Influence of guide stars number and geometry on performance

The effect of the number of LGS on the performance of the GLAO system has been studied. A preliminary study has shown that using more than 4 LGS is useless in terms of GLAO performances that, at the contrary, are negatively affected in the cases of asterism having less than 3 guide stars. Figure 1 (left) shows that passing from 3 to 4 laser guide stars improves the behavior of the system only marginally in term of energy concentration with minor influence on the PSF uniformity.

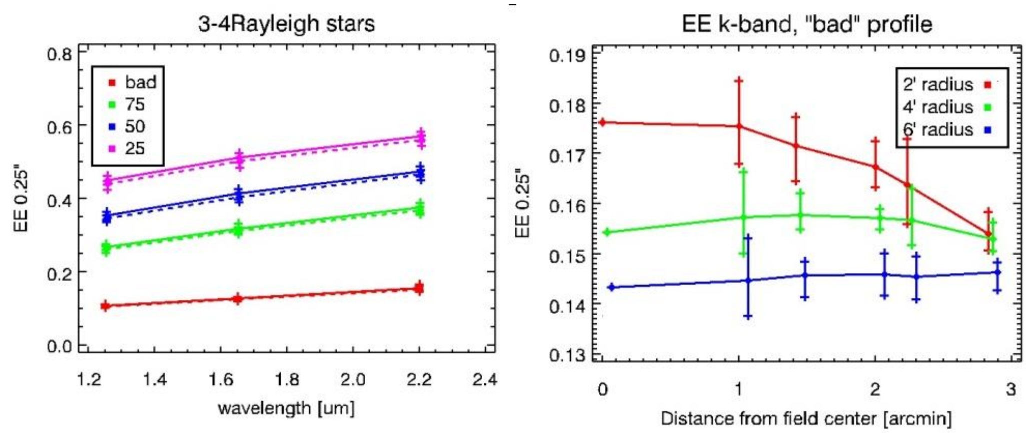

Figure 1 Left: EE for a GLAO system using 4 LGS (solid) or 3 LGS (dashed). Right: EE vs. distance from the center of the asterism for LGS arranged on a circle of radius 2’ (red), 4' (green), 6' (blue

The radial geometry of the asterism seems to have a bigger impact on performances: 3 cases have been studied, with LGS arranged on a circle of radius 2', 4' and 6'. Figure 1 (right) shows the PSF uniformity as a function of the distance from the field center: a 2' radius asterism will provide better performances in term of on-axis resolution and concentration with respect to the 4' radius case, but this is obtained at the expenses of PSF uniformity. On the other hand, widening the asterism to 6' radius reduces the EE without increasing the uniformity.

2.3 Dependency on return flux from LGS and NGS

The dependency of GLAO correction on return flux from LGS and from NGS has been addressed simulating three distinct cases as reported in Figure 2. Laser power has been computed supposing a telescope located at 3500m above sea-level, 4 Rayleigh beacons gated 100m at 12000m above the telescope. The system has 15x15 subapertures, an overall efficiency (optics transmission and Q.E. of detector) equal to 0.25 and 1ms of integration time. NGS R-magnitude has been estimated supposing 5ms integration time on the TT WFS.

Figure 2 shows the FWHM of the PSF corrected by the GLAO system in the three cases described above.

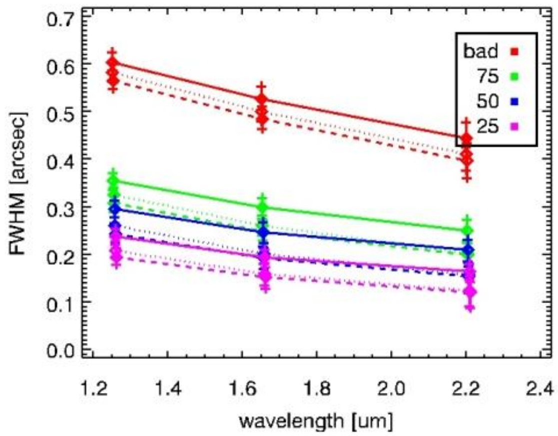

	LGS		NGS	
	ph/subap @ 1ms	Laser (W)	ph/subap @ 5ms	R-mag
Dashed	1000	30	10k	12
Dotted	100	3	10k	12
Solid	100	3	20	19

Figure 2: Dependency of GLAO correction on return flux from LGS and NGS. The table describes the solid, dotted and dashed cases. A bright tip-tilt star has a larger influence than increasing the laser return from 100 to 1000 photons.

2.4 Conclusions

Figure 3 shows synthetically the performance of the simulated GLAO system using a constellation of 4 LGS at 12km and 3 NGS arranged on a 4arcmin radius circle in the “bright” regime (30W laser, NGS 12Rmag).

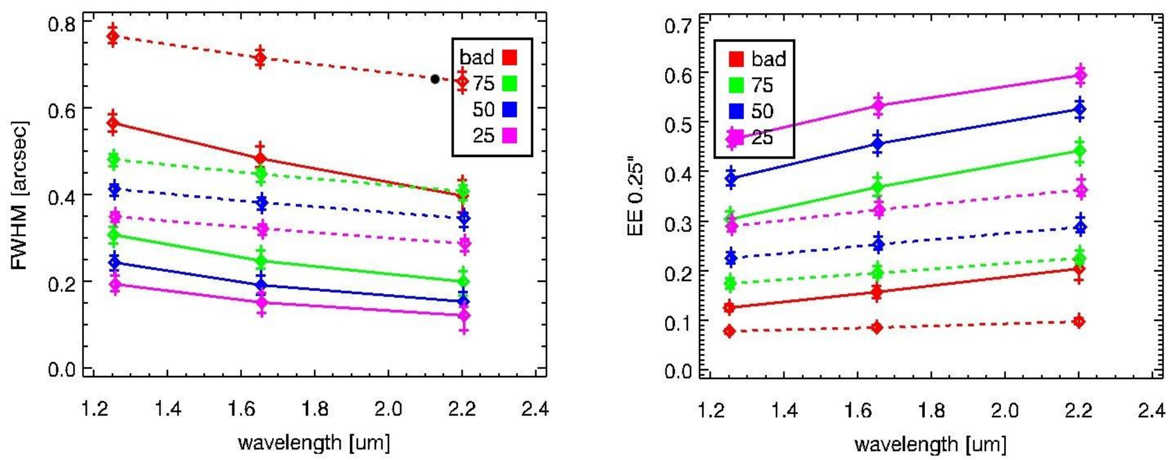

Figure 3: Overall performance of the GLAO system in the baseline configuration described in the text. Solid lines refer to GLAO correction; dashed lines refer to the uncorrected case.

The following points summarize the most important results of the simulations:

- The GLAO system in the baseline configuration assumed in this chapter is able to improve both the PSF FWHM and the EE from J to K band of a factor between 1.5 and 3 mainly depending on turbulence profile.

- Using 3 instead of 4 LGS does not impact the performance. A system with 4 LGS will eventually face the malfunctioning of one laser beam without any appreciable performance loss.

3. WFS OPTICAL DESIGN

This section describes the optical design of the GLAO WFS for the 12 km altitude Rayleigh stars. We assume that the system will make use of 4 laser beams but everything in the design can be converted to the 3 guide star case with minor modifications.

3.1 Pickoff optics to split the LGS beams from the scientific field

A central issue is related to the choice of the optical element used to deflect the return laser flux toward the GLAO WFS. Two possible solutions are envisioned: a set of 4 pick-off mirrors (one per laser beam) or a tilted dichroic plate. Both solutions present drawbacks that pose constrains on the angular radius of the LGS asterism: the coating quality of the dichroic limit its size to a maximum off-axis angle of 2 arcmin. On the other side, the pick-off mirrors must be placed far enough from the optical axis to prevent vignetting of the LUCIFER field of view and this constrains the pick-off mirrors solution to use asterisms wider than 5 arcmin resulting in a loss of return flux caused by the vignetting of the laser beams on the tertiary mirror (M3). The bottom line of it is that the asterism size has only 2 possible values: either 2 arcmin using a dichroic plate in front of LUCIFER or 5 arcmin using pick-off mirrors. The choice among this 2 configurations is still under debate.

The feeding optics are placed in front of the derotator of the LUCIFER focal station. The beams are directed towards the currently unused adjacent focal station that offers the appropriate space for the WFS. A 3D view of a possible arrangement of the WFS optomechanics in the mechanical structure of the telescope is shown in Figure 4 where pickoff mirrors are used as feeding optics. A similar mount can also hold the dichroic plate. The green box on the left of the picture encloses the WFS optics. The envelope of the WFS unit spans approximately 1000mm in length, from the first optical element to the focal plane of the SH sensor.

The optics of the WFS is designed to use guide stars in the range 2-6 arcmin distance from the center FoV. In the following analysis we will describe the WFS design for a star constellation of 5 arcminutes radius.

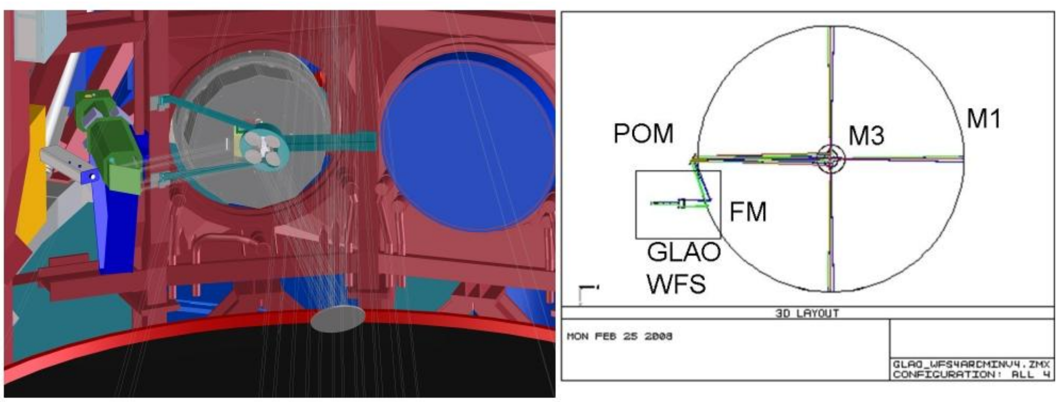

Figure 4 Left: A CAD view of the WFS optomechanics attached to the LBT telescope structure. The green box on the left side of the picture is the enclosure of the WFS optics. The pick off optical elements (mirrors in this sketch) are mounted to a structure being removable if required for aluminization of the primary. Right: The layout of the LBT optical train together with the GLAO WFS optics.

3.2 GLAO WFS optical design

The WFS optics is arranged in such a way that a single CCD with a single lenslet array can be used to provide four SH sensors at the same time. In this way the multiple star sensor unit is quite compact and a single CCD can be used for all the WFS. In the foreseen optical configuration each of the 4 SH sensor has 15x15 subapertures across the LBT pupil.

A more detailed view of the GLAO WFS optics is reported in Figure 5.

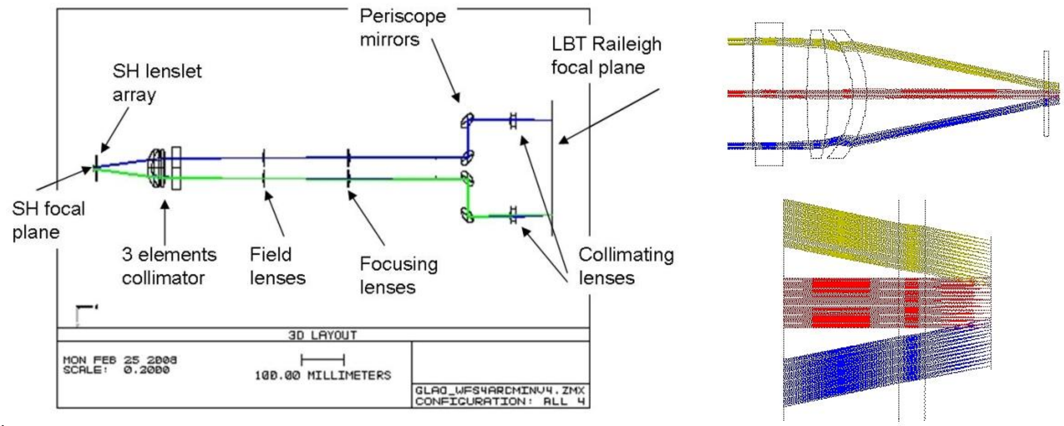

Figure 5 Left: A view of the optical design of the GLAO WFS. Total track of the system along the Z axis is 1000mm while the dimension perpendicular to the Z axis is 350mm. Right: Detail of the beam propagation in the collimator (top) and after the SH lenslet array (bottom). A single CCD is placed in the lenslet focal plane to sample the four spot patterns.

The main characteristics of the WFS optics are the following:

- The periscope assembly allows to image the four stars in a range of 2-6 arcminutes radius from the center with a moderate size collimator.
- A single CCD is used to sample the four SH spot patterns.
- A space of 260mm is available in between the periscope and the focusing lens for polarizers and Pockels cells used to range gate the laser beam. At this position the beams are collimated and parallel to the mechanical axis to keep a good extinction ratio of the Pockels cells.
- Laser beam jitter due to atmospheric perturbations is corrected using the first folding mirror of the periscope. These folding mirrors are conjugate to the LBT telescope pupil. The pupil diameter at this location spans approximately 5mm.

The planned plano-convex lenslet array has a lenslet pitch of 0.408mm and a focal length of 7.5mm. The telescope pupil is therefore sampled nominally with 15x15 subapertures. The actual number of subapertures is slightly reduced due to the vignetting effect occurring at the tertiary mirror. The SH lenslet F# is 18.2. In this configuration the SH plate scale amounts to 65 microns per arcsec. The spot pattern can be properly sampled using a CCD with a pixel size of 51 microns and 256x256 pixels. With this CCD we have a ratio of 0.78 arcsec/pixel and each spot is sampled by 8x8 pixels per subaperture corresponding to a 6.25 arcsec FoV. The single spot optical quality is 20 micron or 0.29 arcsec. The diffraction FWHM in this case is 9.6 micron at a wavelength of 530nm. The arrangement of the spot pattern on the CCD is reported in Figure 6 below. The four spot patterns are contained in a square area having a side of 12.6mm. The area of the mentioned CCD is a square with a side of 12.8mm. We identified a suitable CCD that is produced by the semiconductor laboratory of MPI having the mentioned characteristics, with full-frame rate of ~1000Hz and a read out noise of 2.5electrons.

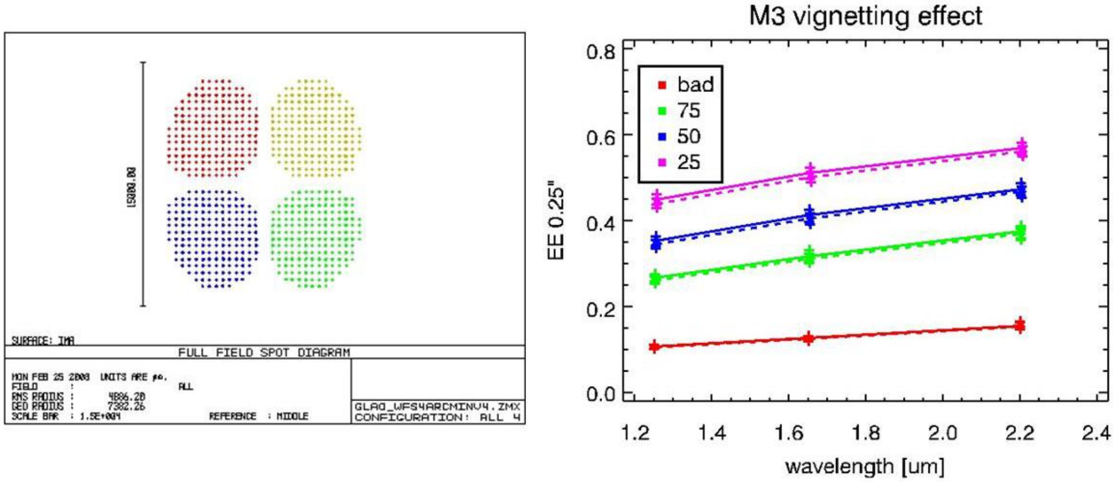

Figure 6. The spot patterns arrangement on the WFS CCD. The spot separation is 0.408mm. The right side of the picture report the GLAO system performance in terms of encircled energy (EE) for the unvignetted (thick lines) and vignetted case (dashed lines)

The plot on the right of Figure 6 shows the performance of the GLAO system with no vignetting and with the M3 vignetting due to the large off-axis angle of the 5 arcmin beacon constellation. The results do not show any significant difference. It has to be noted that each primary sub-aperture is sampled by at least three spots ensuring that the performance is not degraded by this effect. This result is validated by other simulations where only three starts are used. This simulation shows that the 3 star performances are very similar to the four star performance suggesting that some vignetting effect reducing the spot number from 4 to 3 on some of the subapertures do not change the GLAO system performance significantly. Some vignetting occurs as well at the primary mirror, but this contributes only a few %. The M3 vignetting in the 2 considered case (5 and 2 arcmin beacon constellation) is graphically shown in Figure 7 with the four star constellation oriented at 45 degrees with respect to the M3 axis. The major axis sizes of the elliptical M3 mirror are 634mm and 534mm respectively, resulting in a vignetting of 19% for the 5 arcmin constellation and negligible vignetting in the 2 arcmin case.

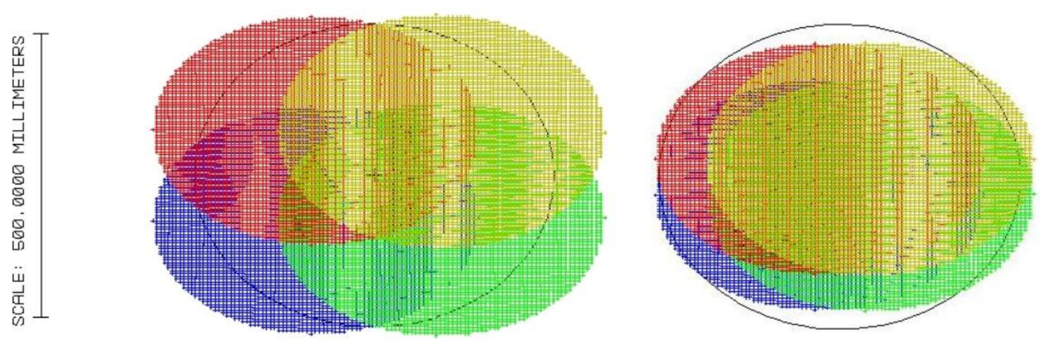

Figure 7 The tertiary mirror with the footprints of the four beams in the case of an off axis angle of 5 arcminutes (left) and 2 arcminutes (right). In the 5 arcmin case the loss of return flux due to M3 vignetting is 19%.

There are a couple of points about the described system that are worth to be mentioned:

- The number of subapertures has not been optimized. Maybe a smaller number of subapertures (12x12) could be used allowing for changing the 256x256 pixel CCD with a 128x128pixel camera.
- The system is designed to work with four reference stars. However the optical design could be easily adjusted to work with three stars if found beneficial.

4. A LOW POWER SODIUM LASER UPGRADE FOR THE LBT GLAO SYSTEM

In the following we will describe a possible upgrade of the GLAO system that can deliver diffraction limited performance using a low power (2-4W) sodium laser. The proposed system will use both GLAO Rayleigh beacons and low power Sodium beacon simultaneously to sample the ground layer and high layer turbulence respectively. (see [4] and [5])

4.1 Concept

Strong turbulence near the ground is effectively sampled and corrected by a Rayleigh GLAO system, but Rayleigh beacons cannot provide an accurate sampling of the highest atmospheric layers because of the low altitude at which they operate. The uncorrected turbulence of the higher part of the atmosphere dominates the wavefront residual in the case of a plain GLAO system.

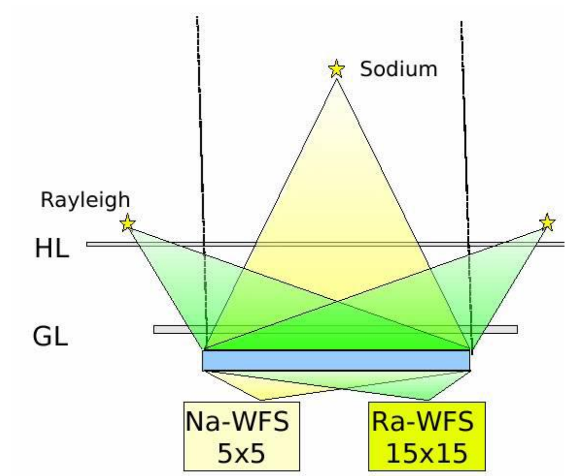

Figure 8 **A** sketch of the arrangement of the proposed sources for the upgrade of the GLAO system. An additional Na WFS is required.

In this section we propose an upgrade of the LBT GLAO system that makes use of a low-power sodium laser to sense the high altitude turbulence. The achieved information is then combined with the information on ground layer turbulence measured by the GLAO WFS. The result is an estimate of the wavefront in the direction of the LGS. We will show with numerical simulation that this estimation is good enough to provide diffraction limit performance within the isoplanatic patch. It is to be noted that, as shown below, the performances of the upgraded GLAO system are substantially equivalent to the performance achieved with a single sodium laser being 3 to 10 times more powerful.

The central point stands in the observation that the turbulence of the high layers, the ones not sampled by the GLAO, is weaker of the ground layer turbulence and can be corrected using a smaller numbers of modes. This allows using larger subapertures that in turn means a reduced return flux to get a sufficient number of photons per frame. A more intuitive way of rephrasing this concept is the following: the strength of the turbulence of the whole atmosphere is proportional to r0 which, as a rule of thumb, sets the subaperture size required to get a given degree of AO correction. We can introduce an effective r0 representing the strength of the turbulence un-sampled by the Rayleigh beacons. This effective r0 will be larger (about a factor 2, as we will see below) than the whole-atmosphere r0. As a consequence, a second wavefront sensor dedicated to the sampling of high layers turbulence can use larger subapertures, hence a fainter guide star. In the case the guide star is a Sodium guide star the required power of the sodium laser, that is roughly inversely proportional to the square of r0, is significantly reduced.

In the simulations shown before, for the ‘25’ and ‘bad’ case after GLAO correction, the un-sampled turbulence due to high layers have rms values of 0.58um and 1.36um, corresponding to r0 values in K band of 4.36m and 1.57m respectively.

As a rough estimate, to correct such a residual turbulence up to a residual error of 0.5rad, we need to sample and correct the high layers with ~20 modes [6]. The effective r0 values and the estimate of the required number of modes to be corrected are summarized in Table 2.

Supposing to correct the high layers turbulence using a 20-modes basis, a WFS with 5x5 subapertures will suffice. Comparing to sodium-only LGS systems, typically having 15x15 subapertures and a laser-power of 20W, one can see that the proposed system increases the area of each subapertures of a factor ~10 and this corresponds to a laser power requirement reduced of the same amount.

Table 2 Each cell contains: (left) the effective r0 [m] of high layers un-sampled by GLAO system and (right) the number of modes that have to be corrected by the high layer sodium AO to reach a residual error of 0.5 rad. in most of the cases (grey boxes) a correction with 20 modes will be enough to achieve diffraction limited performance.

	25	**50**	**75**	**Bad**
J-band	2.2 / 15	1.8 / 23	1.4 / 34	0.8 / 103
H-band	3.1 / 8	2.5 / 12	2.0 / 18	1.1 / 55
K-band	4.4 / 4	3.5 / 7	2.8 / 9	1.6 / 28

4.2 Use of a NGS for high layers correction

It is worth to be noted that the sodium LGS can be in principle substituted by a natural guide star (NGS). The NGS has to be bright enough to correct ~20 modes, and this poses a limit in the sky coverage that can be overcome only by using a Sodium-LGS. On the other hand, the use of a NGS has 2 main advantages over a LGS: the first one is that the NGS does not suffer of focal anisoplanatism, the second one is that the needed hardware will be already available at the LBT, since the NGS pyramid wavefront sensor located in the AGW that will be commissioned in 2009 together with the adaptive secondary mirror will fulfill this task with none or minor modifications.

4.3 Simulated performances

To validate the concept, we simulated a system having one additional wavefront sensor sensing a sodium beacon on-axis at 90km (Na-WFS in the following) and capable of reconstruct the wavefront on a 20 modes basis. The system also has a WFS (GL-WFS in the following) that combines the Rayleigh beacons and reconstructs the ground layer on a 150 modes basis. Finally the system has a NGS tip tilt tracker. In the presented simulation the tilt NGS is considered to be on axis and no measurement noises are taken into account.

The simulated mixed Rayleigh-Sodium system is capable of reaching the diffraction limit in J, H and K bands with every atmospheric model except for the case of J-band and 'bad' profile (see Figure 9). This is coherent with the estimate shown in Table 2, where this last case requires a much higher number of corrected modes to achieve the same degree of correction with respect to the others cases.

The on axis SRs achieved are 10, 25, 45% in J, H, K band respectively for the 50 percentile atmospheric profile. These numbers are comparable with the SR computed in [7] where a single sodium system achieve a SR of 58-37 % in K band and 39-17% in H band for two different atmospheric profiles when tip tilt error is not taken into account.

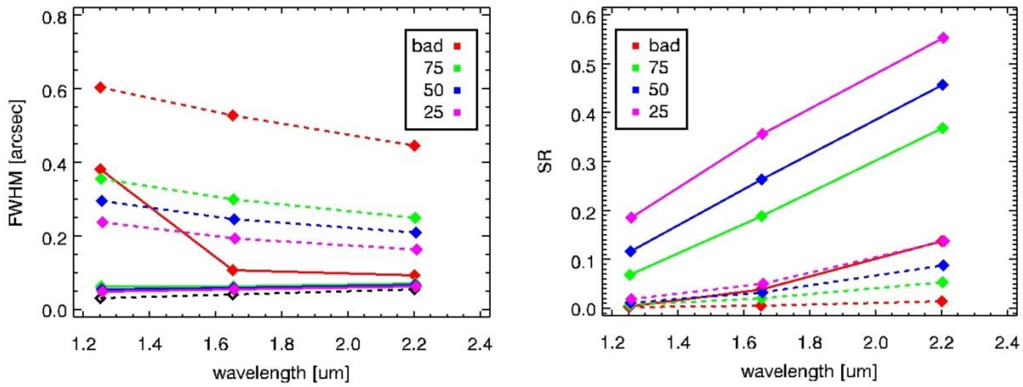

Figure 9 Left: Performances (FWHM of a central field) of the mixed Rayleigh-Sodium system (solid lines) and of the GLAO system (dashed lines). Dashed black line shows the diffraction limit. Right: Performances (SR of a central field) of the mixed Rayleigh-Sodium system (solid lines) and of the GLAO system (dashed lines)

4.4 Preliminary optical design of a 5x5 SH sensor for the upgrade path.

In this section we describes the optical set-up of a low order SH sensor that can be placed at different locations in the LBT telescope to upgrade the Rayleigh GLAO system. A possible arrangement consists in placing the Na-WFS and the NGS tip tilt tracker in the AGW unit. This arrangement is sketched below in Figure 10.

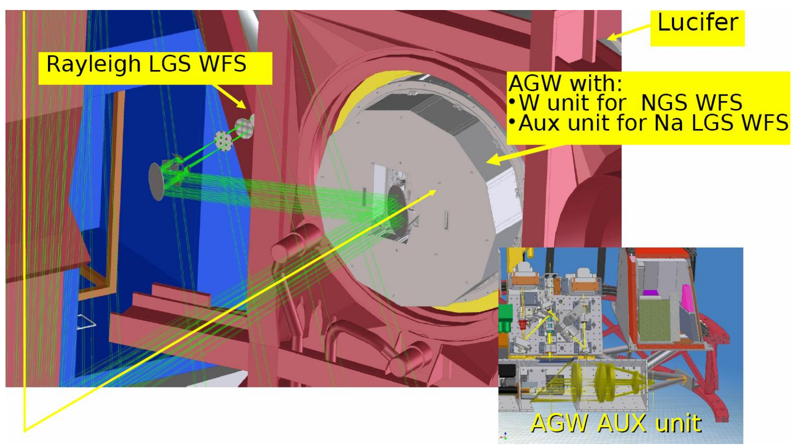

Figure 10 A 3D picture showing the placements of the GLAO WFS and of the upgrade path WFS. The NGS WFS is supposed to be placed in the W unit too. The inset on the lower right shows the placement of the Na-WFS in the W unit auxiliary units bench. The optics shown are dimensioned for a layer oriented tomographic WFS having a FoV of 2'.

The WFS optical arrangement is reported in the left part of Figure 11. Position of pick-off mirror with respect to the LUCIFER window is showed in the right part of Figure 11.

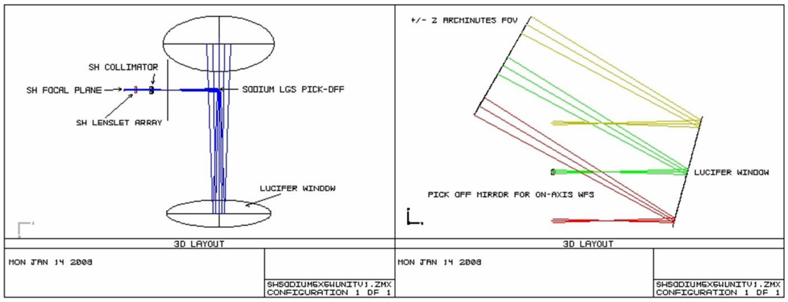

Figure 11. Left: a picture showing the arrangement of the low order WFS in the AGW unit. The reflection on the LUCIFER window is showed. Right: the position of the pick-off mirror with respect to the scientific FoV.

The SH collimator is placed 16mm out from the LUCIFER window so that no additional vignetting is present on the scientific field of LUCIFER. This is showed in the right part of Figure 11 where the arrangement of the LUCIFER window and sodium star pick-off mirror is reported. The SH lenslet array has a focal length of 17.3mm and a pitch of 0.336mm. The lenslet F/# results 51.5. The scale of the SH focal plane is 47 micron per arcsec. The design is matched with a CCD having a pixel size of 24 microns like the EEV chip 80x80 or 128x128. In this case each of the lenslet FoV is sampled with 14x14 pixels and the SH pixel scale results 0.5 arcsec/pixel. The diffraction limited FWHM is found to be 30 micron. The total number of pixels used is 70x70 so that both size of chip could be used.

4.5 Some additional considerations on the upgrade path.

We remark that the Na-WFS could be upgraded to work with multiple sodium guide stars as a tomographic WFS. The WFS could work in the so called star oriented mode or in a layer oriented mode. If a tomographic sensor is used to sample the high altitude layers the Sodium beacon focus anisoplanatism could be eliminated so increasing the on-axis Strehl ratio of the system. Moreover removal of focus anisoplanatism would improve the system performance at short wavelength like J band where the achieved SR is 10 % in our simulation. A single-layer layer-oriented WFS will require to split the same low power sodium in multiple sources and recombine them in the SH focal plane. A slightly different optical system is required in this case for the WFS. This tomographic optical design can work with a single star and with multiple star with the same optics. The space needed is such that the designed layer oriented WFS could be placed in the auxiliary unit bench of the W unit as considered for the single source SH sensor. Finally in the case of available high-power sodium laser, a full tomographic version of this layer oriented WFS having two or three conjugated planes could be realized using only Sodium beacons.

REFERENCES

[1] S. Rabien et al. “The Laser Guide Star program for the LBT”, Proc SPIE (2008)
[2] CAOS http://www-luan.unice.fr/caos
[3] ForOt http://forot.arcetri.astro.it
[4] G. Brusa et al. "A study for a multi-conjugate AO system for 8m class telescopes", in Laser Weapons Technology, T. D. Steiner and P. H. Merritt, eds., Proc. SPIE 4034, 190–200 (2000)
[5] I. A. De La Rue and B. L. Ellerbroek, "Multi Conjugate adaptive optics with hybrid laser beacon systems", in Adaptive Optics Systems and Technology II, Robert K. Tyson; Domenico Bonaccini; Michael C. Roggemann, eds, Proc SPIE 4494, 290-301 (2002)
[6] R. J. Noll ”Zernike polynomials and atmospheric turbulence”, JOSA 66, 3 207-211 (1976)
[7] D. G. Sandler et al. “Adaptive optics for diffraction-limited infrared imaging with 8-m telescopes”, JOSA A, 11, 2 925-946, (1994)